IJC
International Journal of Cancer

Expression profiling shows differential molecular pathways and provides potential new diagnostic biomarkers for colorectal serrated adenocarcinoma

Pablo Conesa-Zamora[1]*, José García-Solano[1]*, Francisco García-García[2], María del Carmen Turpin[1,3], Javier Trujillo-Santos[4], Daniel Torres-Moreno[1], Isabel Oviedo-Ramírez[1], Rosa Carbonell-Muñoz[5], Encarnación Muñoz-Delgado[6], Edith Rodriguez-Braun[7], Ana Conesa[2] and Miguel Pérez-Guillermo[1]

[1] Department of Pathology, Santa Lucía General University Hospital (HGUSL), Cartagena, Spain
[2] Department of Bioinformatics and Genomics, Centro de Investigación Príncipe Felipe (CIPF), Valencia, Spain
[3] Francisco de Vitoria University, Madrid, Spain
[4] Department of Internal Medicine, HGUSL, Cartagena, Spain
[5] Department of Clinical Analysis, HGUSL, Cartagena, Spain
[6] Department of Biochemistry and Molecular Biology-A, University of Murcia, Murcia, Spain
[7] Department of Clinical Oncology, HGUSL, Cartagena, Spain

Serrated adenocarcinoma (SAC) is a recently recognized colorectal cancer (CRC) subtype accounting for 7.5 to 8.7% of CRCs. It has been shown that SAC has a poorer prognosis and has different molecular and immunohistochemical features compared with conventional carcinoma (CC) but, to date, only one previous study has analyzed its mRNA expression profile by microarray. Using a different microarray platform, we have studied the molecular signature of 11 SACs and compared it with that of 15 matched CC with the aim of discerning the functions which characterize SAC biology and validating, at the mRNA and protein level, the most differentially expressed genes which were also tested using a validation set of 70 SACs and 70 CCs to assess their diagnostic and prognostic values. Microarray data showed a higher representation of morphogenesis-, hypoxia-, cytoskeleton- and vesicle transport-related functions and also an overexpression of fascin1 (actin-bundling protein associated with invasion) and the antiapoptotic gene hippocalcin in SAC all of which were validated both by quantitative real-time PCR (qPCR) and immunohistochemistry. Fascin1 expression was statistically associated with *KRAS* mutation with 88.6% sensitivity and 85.7% specificity for SAC diagnosis and the positivity of fascin1 or hippocalcin was highly suggestive of SAC diagnosis (sensitivity = 100%). Evaluation of these markers in CRCs showing histological and molecular characteristics of high-level microsatellite instability (MSI-H) also helped to distinguish SACs from MSI-H CRCs. Molecular profiling demonstrates that SAC shows activation of distinct signaling pathways and that immunohistochemical fascin1 and hippocalcin expression can be reliably used for its differentiation from other CRC subtypes.

Serrated adenocarcinoma (SAC) has been recently recognized in the latest WHO classification of tumors of the digestive system as a new subtype of colorectal cancer (CRC).[1] Criteria for its histological diagnosis have been proposed[2,3] and recently validated in a series of 81 cases,[4] its frequency ranges from 7.5 to 8.7% of all CRCs[4,5] and it has been shown to have a worse prognosis than conventional carcinoma (CC).[4] Accordingly, SAC displays a higher frequency of adverse

Key words: serrated adenocarcinoma, microarray analysis, fascin, hippocalcin, colorectal cancer, microsatellite instability

Abbreviations: AUC-ROC: area under receiver operating characteristic curve; CC: conventional carcinoma; CIMP: CpG island methylation phenotype; CRC: colorectal carcinoma; EMT: epithelial-mesenchymal transition; GO: gene ontology; GSA: gene set enrichment analysis; hMSI-H CRC: colorectal carcinoma displaying histological features of high-level microsatellite instability; HR: hazard ratio; IHC: immunohistochemistry; MSI: microsatellite instability; MSI-H: high-level MSI; MSI-L: low-level MSI; MSS: microsatellite stability; qPCR: quantitative polymerase chain reaction; SAC: serrated adenocarcinoma; SD: standard deviation; WHO: World Health Organization

Additional Supporting Information may be found in the online version of this article.

*P.C.-Z. and J.G.-S. contributed equally to this work

Grant sponsor: Seneca Foundation; **Grant number:** 08768/PI/08; **Grant sponsor:** Instituto de Salud Carlos III, Ministerio de Sanidad, Spain; **Grant number:** P1081210; **Grant sponsor:** MICINN; **Grant number:** BIO2009-10799

DOI: 10.1002/ijc.27674

History: Received 26 Mar 2012; Accepted 1 Jun 2012; Online 14 Jun 2012

Correspondence to: Pablo Conesa-Zamora, Department of Pathology, Santa Lucía General University Hospital (HGUSL), C/Mezquita s/n. 30202, Cartagena, Spain, Tel.: +34-96-812-8600, Fax: +34-96-832-6389, E-mail: pablo.conesa@carm.es

What's new?

Serrated adenocarcinoma (SAC), a recently recognized colorectal cancer subtype, was shown in a previous study to possess unique molecular and immunohistochemical features. Here, microarray and immunohistochemical analyses of tissue samples from SAC patients with dissimilar environmental and genetic backgrounds validates these features. Fascin1, which is associated with tumor cell invasion, and the antiapoptotic gene hippocalcin were identified as potential biomarkers of SAC, and hence may be valuable immunohistochemical adjuncts in SAC diagnosis.

histological features at the invasive front including high-grade tumor budding and cytoplasmic pseudofragments, infiltrating growth pattern, and weak peritumoral lymphocyte response.[6] More recently, an immunohistochemical study on adhesion molecules has demonstrated a different expression pattern of SAC compared with CC[7] and, in another study, SAC differed from CRC displaying histological features of high-level microsatellite instability (hMSI-H CRC) in terms of *KRAS* and *BRAF* mutation prevalence, MSI status, and MLH1 expression.[2,8,9]

A two-arm model has been proposed to explain the progression of the serrated pathway, the aberrant crypt foci-hyperplastic type being the earliest lesion which may develop into hyperplastic polyps and sessile serrated adenomas, or into traditional serrated adenomas (TSA), both of which may progress to SAC. However, this pathological pathway is not entirely lineal since TSA has also been considered as precursor of CC.[1] Cancers developing from these lesions may show high- or low-level microsatellite instability (MSI-H and MSI-L, respectively) or may be microsatellite stable (MSS).[10] In this pathway, inhibition of apoptosis and subsequent inactivation of DNA repair genes by promoter methylation seem to play an important role.[1,5]

Based on earlier reports,[8] it appears that SAC is a heterogeneous entity at the molecular level sharing some features with CC (high frequency of *KRAS* mutation), whereas in other respects (*BRAF* mutation, CpG island methylation phenotype (CIMP) affecting DNA repair genes and MSI) its features are typical of sporadic microsatellite unstable carcinoma.[5,8,9,11] Little is known about SAC tumor biology and to date there has been only one study of the gene expression profile of SAC showing that morphogenesis, hypoxia response and membrane-associated genes seem to be upregulated.[12]

In this study, we have analyzed the molecular profile of SAC with the aim of:

- Evaluating the distinct aberrant biological functions of SAC and comparing them with earlier studies and with a previous molecular profiling in which a different microarray platform was used.[12]
- Validating the genes differentially expressed in SAC in comparison with those expressed in CC at the mRNA and protein level.
- Analyzing possible diagnostic and prognostic value of the proposed markers.
- Studying the presence of the identified biomarkers in hMSI-H CRC and comparing them with those found in SAC.

Material and Methods

Patients and tumor samples

The clinicopathological features of the patients have been previously reported.[4,6] Updated follow-up information was obtained from cancer registry files and approval for the study was granted by the Local Ethical Board. SACs were diagnosed on the basis of criteria proposed by Mäkinen[5] and CCs according to prior established criteria.[13] Frozen samples of 11 SACs were retrieved from the biobank of our institution for gene expression profiling. In addition to serrated morphology, 1 of 11 SACs displayed poorly-differentiated areas and 7 showed a mucinous component. Frozen samples of 15 CC were selected as a control group from the same tumor bank. Paraffin blocks of 70 SAC, 70 CC, and 20 hMSI-H CRC cases, included in previous reports,[8] were available for immunohistochemical validation of microarray results. Clinicopathological features of the cases are shown in Table 1.

Twenty hMSI-H CRC cases were selected from a series of 220 consecutive CRC diagnosed in the period 2008 to 2011 based on the presence of MSI-H histological features (mucinous, signet-ring cell, and medullary carcinoma, tumor infiltrating and peritumoral lymphocytes, "Crohn-like" inflammatory response, poor differentiation, tumor heterogeneity, and "pushing" tumor border).[14] Mean age was 66.8 (SD $\pm$13.9), 65% were female, 95% were proximally located, Dukes' stage was A: 5%, B: 40%, C: 55%, all were WHO low-grade and in 10% the mucinous component exceeded 50%. MSI analysis demonstrated that all were MSI-H[8] and none of the 20 hMSI-H CRC displayed serrated morphology.

RNA extraction

A volume of approximately 10 mm^3 was extracted from each frozen tissue using the disposable sterile biopsy punch Acupunch 2 mm (Acuderm Inc., Lauderdale, FL). RNA was extracted following the manufacturer's instructions (Qiagen, Hilden, Germany). Briefly, tissue was disrupted and homogenized in 700 μl of Qiazol (Qiagen ref: 1023537) using a Tissueruptor by Qiagen for 20 sec. The homogenate was incubated at room temperature for 5 min. After adding 140 μl of chloroform and centrifuging at 12,000*g* for 15 min at 4°C, 350 μl of the aqueous phase was subjected to automatic total

Table 1. Demographic and pathological features of the study cases

	Training set			qPCR validation set			IHC validation set		
	SAC, $n = 11$ (%)	CC, $n = 15$ (%)	p	SAC, $n = 18$ (%)	CC, $n = 25$ (%)	p	SAC, $n = 70$ (%)	CC, $n = 70$ (%)	p
Gender									
Female	5 (45.5)	8 (53.3)		9 (50)	13 (52.0)		36 (51.4)	37 (52.9)	
Male	6 (54.5)	7 (46.7)	0.691	9 (50)	12 (48.0)	0.897	34 (48.6)	33 (47.1)	0.866
Age [SD]	65.1 [22.4]	68 [10.2]	0.660	65.8 [9.7]	67.4 [14.3]	0.683	67.6 [13.6]	68.5 [13.5]	0.951
Location									
Proximal	9 (81.8)	9 (60.0)		10 (55.6)	12 (48.0)		39 (55.7)	37 (52.9)	
Distal/rectum	2 (18.2)	6 (40.0)	0.234	8 (44.4)	13 (52.0)	0.625	31 (44.3)	33 (47.1)	0.734
Dukes' stage									
A	3 (27.3)	3 (20.0)		3 (16.7)	4 (16.0)		8 (11.5)	8 (11.4)	
B	1 (9.1)	2 (13.3)		5 (27.8)	8 (32.0)		26 (37.1)	28 (40.0)	
C	7 (63.6)	10 (66.7)	0.881	10 (55.6)	13 (52.0)	0.956	36 (51.4)	34 (48.6)	0.937
WHO grade									
High	1 (9.1)	1 (6.7)		1 (5.6)	1 (4.0)		5 (7.1)	3 (4.3)	
Low	10 (90.9)	14 (93.3)	0.819	17 (94.4)	24 (96.0)	0.811	65 (92.9)	67 (95.7)	0.467
Type									
Nonmucinous	4 (36.4)	4 (26.7)		12 (66.7)	21 (84.0)		55 (78.6)	60 (85.7)	
Mucinous	7 (63.6)	11 (73.3)	0.597	6 (33.3)	4 (16.0)	0.184	15 (21.4)	10 (14.3)	0.270

Abbreviations: SAC: serrated adenocarcinoma; CC: conventional carcinoma; qPCR: quantitative polymerase chain reaction; IHC: immunohistochemistry; SD: standard deviation; WHO: World Health Organization.

RNA extraction using the Qiacube equipment and the miRNeasy Mini Kit (ref: 217004), both provided by Qiagen.

RNA labeling and microarray hybridization

Total RNA was quantified by spectrometry (NanoDrop ND1000, NanoDrop Technologies, Wilminton, DE) and fragment size distribution was analyzed by RNA 6000 Pico Bioanalyzer assay (Agilent Technologies, Palo Alto, CA). RNA (150 ng) was concentrated in a SpeedVac to a working dilution and used to produce cyanine 3-CTP-labeled cRNA using the Low Input Quick Amp Labeling Kit, One-Color (Agilent p/n 5190-2305) according to the "One-Color Microarray-Based Gene Expression Analysis" protocol Version 6.0 (Agilent p/n G4140-90040). This method uses T7 RNA polymerase which simultaneously amplifies target material and incorporates cyanine 3-labeled-CTP. A 2,000 ng cRNA product was hybridized with Whole Human Genome Oligo Microarray Kit (Agilent p/n G2519F-014850) containing 41,000+ unique human genes and transcripts. Arrays were scanned in an Agilent Microarray Scanner (Agilent G2565BA) according to the manufacturer's protocol and data extracted using Agilent Feature Extraction Software 10.7.1 following the Agilent grid template 014850_D_F_20100430 protocol GE1_107_Sep09 and the QC Metric Set GE1_QCMT_Sep09.

Microarray data analysis

Agilent raw data were preprocessed using Agilent background correction and quantile normalization was applied to obtain homogeneous scales in all samples. Differential expression analysis was performed on normalized data using the Linear Models for Microarray Data (Limma) package by Bioconductor (available at: www.bioconductor.org/packages/2.3/bioc/html/limma.html) and comparison was made between SAC ($n = 11$) and CC ($n = 15$). The p values were corrected by multiple testing using the Benjamini and Hochberg method[15] to give adjusted p values. In order to further identify cellular function differences between SAC and CC, gene expression data were analyzed by Gene Set Enrichment Analysis (GSA) using the FatiScan tool of the Babelomics suite (available at: www.babelomics.org).[16] This methodology looks for sets of functionally related genes that show a coordinated expression behavior. GSA is a functional profiling methodology that relies on the coordinated behavior of sets of functionally related genes rather than on the selection of a number of differentially expressed genes. We used different functional annotation databases, namely the pathways from the KEGG database (available at: www.genome.jp/kegg) and the Biological Process, Molecular Function and Cellular Component from Gene Ontology (GO) (available at: www.geneontology.org). KEGG pathway results were represented by a network from Cytoscape software.(available at: http://www.cytoscape.org/). Each node represents a pathway whose size is associated with the number of genes included in this pathway and the thickness of the connection represents the number of genes shared between two nodes.

Quantitative real-time PCR (qPCR) for mRNAs

cDNAs from 18 SACs and 25 CCs including those used in the training set were included for the qPCR validation of the technique. Information on qPCR experiment is provided as Supporting Information S1.

Immunohistochemistry

The validation subset consisted of 70 SACs and 70 CCs matched for gender, age, location, Dukes' stage and grade and an additional subgroup of 20 hMSI-H CRC was also included. A representative area of each tumor was selected by one of us (J.G.-S.) for a tissue microarray construction as previously described.[7] Details of manufacturers, codes, antigen retrieval conditions, dilutions and clones are provided as Supporting Information S1. Whole 2.5 μm sections and the TMA were incubated with the panel of antibodies: fascin1, hippocalcin, β-dystroglycan and neuronal apoptosis inhibitory protein (NAIP) after confirming a homogeneous tumor cell staining in whole-tissue sections. From the study cases a randomized subset of 39 SACs, 32 CCs and 18 hMSI-H CRC was used to evaluate the expression of NAIP.

Immunohistochemical assessment was done without knowledge of histological diagnoses.

For fascin1, diffuse cytoplasmic staining in epithelial tumor cells was considered a positive reaction (Figs. 1*a*–1*c*) whereas for hippocalcin, NAIP (Figs. 1*d*–1*i*) and β-dystroglycan (Supporting Information S2), granular cytoplasmic staining at the luminal border was considered positive. Immunohistochemical expression of fascin1 in vascular endothelium was considered an internal positive control whereas the absence of expression in normal mucosa as a negative. For hippocalcin and NAIP, paraffin-embedded cerebellum histological sections were used as positive controls and, for β-dystroglycan, paraffin-embedded kidney sections.

Staining scores for these markers were calculated by multiplying the staining intensity score (0 = no staining, 1 = weak or moderate, 2 = strong) in a given tumoral area by the stained area score (1< one-third, 2 = between one- and two-thirds, 3> two-thirds) as previously described.[17] The total immunohistochemical score (0–6) was expressed as the product of the intensity and area scores. Staining was considered positive when the score was ≥ 1. Immunohistochemical procedures and evaluation of MGMT was preformed as we previously reported.[8]

MSI status and oncogene mutation analysis

DNA from the paraffin-embedded tissues included in the immunohistochemical validation set was extracted and analyzed for MSI status and *BRAF*, *KRAS* and *PIK3CA* mutation occurrence as we previously reported.[8]

Statistical and survival analysis

Statistical analysis was performed using Epidat (Version 3.1, Spain) and SPSS (Version 15.0, Chicago, IL) packages. The Pearson's χ^2 test was used for testing associations for statistical significance. Performance tests and the area under receiver operating characteristic curve (AUC-ROC) were calculated for assessing the value of immunohistochemical and molecular parameters as SAC diagnostic markers. The parameters analyzed were the immunostaining score of fascin1, hippocalcin, β-dystroglycan and the previously reported immunohistochemical results of MGMT.[8]

Univariate survival analysis was performed according to the Kaplan–Meier method using the log-rank test for statistical significance. Patients who died within the postoperative period (<1 month) were excluded from this analysis. Cox regression model was used for multivariate analysis considering $p < 0.05$ as inclusion and $p > 0.10$ as exclusion criteria in a stepwise forward procedure. The parameters considered for survival analysis using the proportional-hazard regression Cox model were diagnosis (SAC *vs.* CC and SAC *vs.* hMSI-H CRC) age, gender, tumor location (proximal *vs.* distal/rectal), Dukes' stage (C *vs.* A/B), fascin1, hippocalcin and β-dystroglycan immunostaining patterns (positive *vs.* negative).

Results

No significant differences were observed in terms of demographic and clinicopathologic features between SAC and CC for the training and validation sets included in the study (Table 1). RNA quality assay showed that all 11 SACs and 15 CC showed a RNA integrity number (RIN) > 6.5 and were optimal for labeling and hybridization onto the microarray.

Differentially expressed functions

GSA revealed significant enrichment of 103 KEGG pathways when comparing SAC and CC gene expression profiles (Supporting Information S3A). As shown in Figure 2, KEGG pathways enriched in SAC samples included apoptosis (hsa04210); morphogenesis (Notch signaling pathway (hsa04330)), VEGF pathway (hsa04370); cytoskeletal organization at membrane junctions (Gap junction (hsa04330), adherens junctions (hsa04520)); DNA repair and synthesis (pyrimidine metabolism (hsa00240), DNA replication (hsa03030), nonhomologous end-joining (hsa03450), base excision repair (hsa03410), folate biosynthesis (hsa00790)); B-cell response (B-cell receptor signaling (hsa04662), Fc epsilon RI signaling (hsa04662), Fc gamma R-mediated phagocytosis (hsa04666)); growth factor receptor signaling (ErbB signaling pathway (hsa04012), mTOR signaling pathway (hsa04150)) and lipid and protein metabolism whereas functions overexpressed in CC were mainly associated with immune response either in xenograft rejection (allograft rejection (hsa05330), graft-*versus*-host disease (hsa05332)) or in autoimmune diseases (autoimmune thyroid disease (hsa05320), Type I diabetes mellitus (hsa04940)).

As regards the Gene Ontology (Supporting Information S3B) GO biological process database, a large number (306) of GO terms were found significantly enriched between SAC and CC. In order to retain high confident enriched function, we selected those for which gene expression differences were

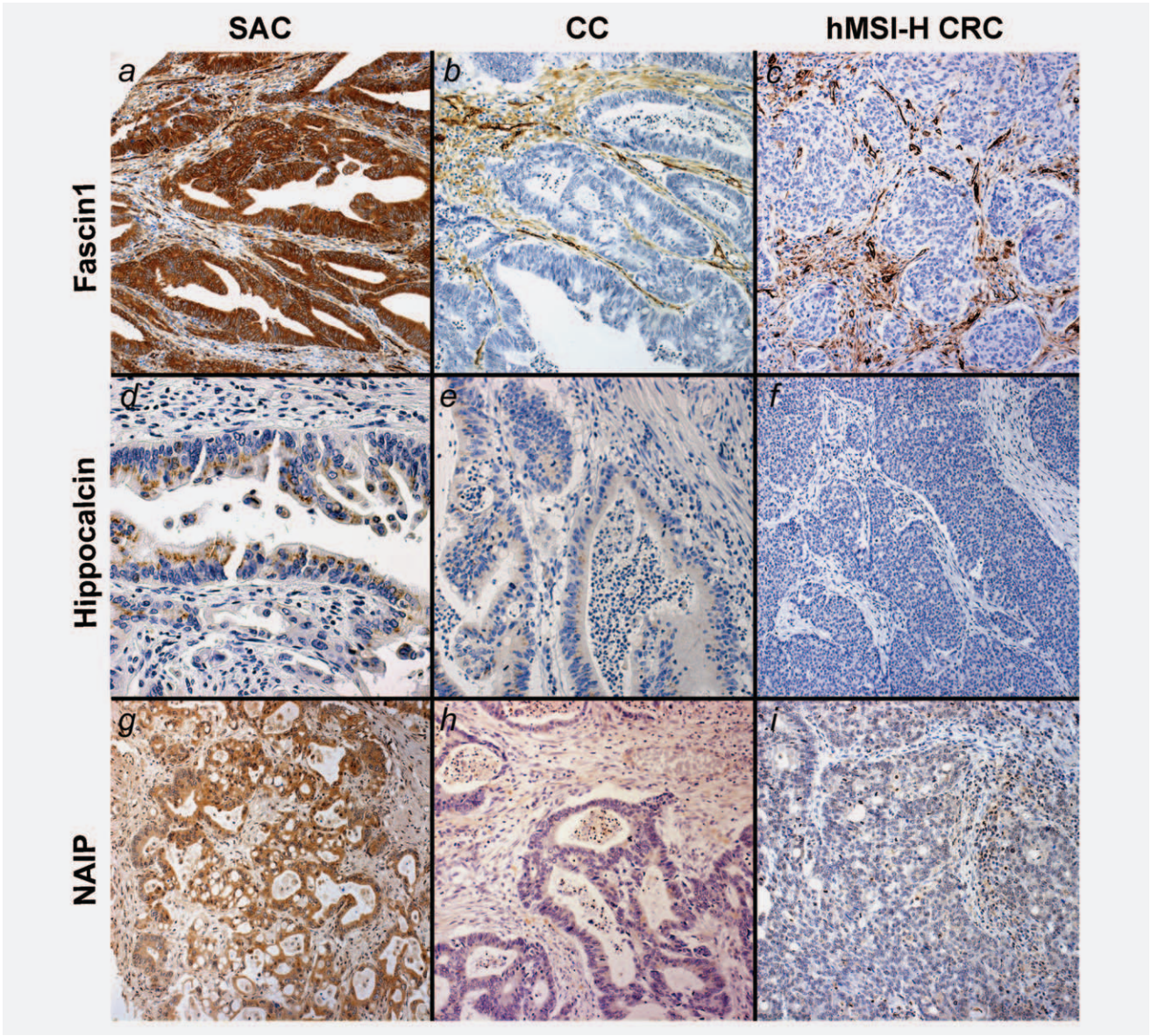

Figure 1. Immunohistochemical expression of fascin1 (*a–c*), hippocalcin (*d–f*) and NAIP (*g–i*) in SAC (first column), CC (second column) and MSI-H CRC (third column); ×20 magnification in all except in *d* (×40). [Color figure can be viewed in the online issue, which is available at wileyonlinelibrary.com.]

larger by restricting them to functions enriched at either the 0.04 or 0.96 percentile position of the ranking of gene expression differences between SAC and CC. After such filtering, 19 functions obtained were overrepresented in SAC. Most of them were related to vesicle transport (four), morphogenesis (three), neuronal markers (two), mesenchymal to epithelial transition (one), negative regulation of IL-12 (one), DNA methylation (one), ion channel (one) and the transforming growth factor β receptor (TGFR) pathway (one). As regards the GO molecular function database, 248 GO terms were differentially enriched between SAC and CC, achieving statistical significance while only 21 terms remained after high confidence filtering as being overrepresented functions in SAC which were to a major extent related to transport of vesicle and ion channel (six), RAS-related GTPases (two), TGFR (one) and carbohydrate metabolism.

Finally, 85 high confidence enriched (<0.05 threshold >0.95) GO cellular component functions (175 total significant terms) were obtained. In SAC, most of them were related to membrane (14) vesicle (20), cytoskeleton (14), neuronal structures (6) and growth factor pathways (6).

Differentially expressed genes and validation by qPCR and immunohistochemistry

The analysis of mRNA expression profiles identified 15 differentially expressed mRNAs, 13 of which were overexpressed and the other two were downregulated in SAC compared with CC (Table 2). Differentially expressed genes included

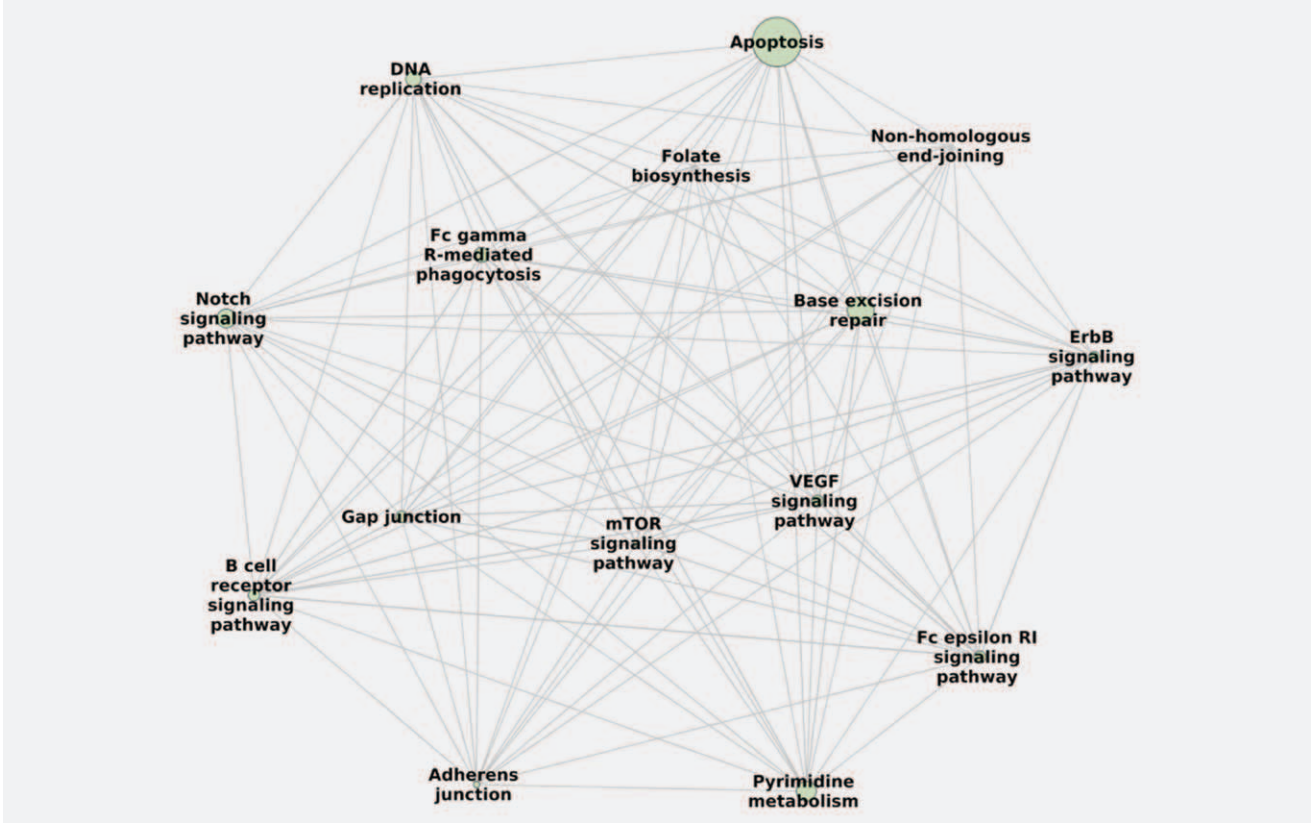

Figure 2. Network of selected significant KEGG pathways differentially represented in SAC compared with CC.

several zinc-finger (*INSM1, ZDHHC12, ZNF329*); cytoskeleton (*FSCN1, DAG1*); Ca^{2+} binding (*HPCA, TTYH3*); and transport proteins (*SLC27A4*) as well as noncoding RNAs.

Based on the differential change of mRNA expression, the importance of the biological functions and the availability of antibodies, we decided to validate the mRNA and protein expression of fascin1 (*FSCN1*), hippocalcin (*HPCA*), and dystroglycan1 (*DAG1*) genes. Consistent with the expression microarray results, qPCR showed that fascin1 and hippocalcin had significantly greater expression in SAC than in CC (*FSCN1*: 7,456.6 copies/million copies of β-*actin* gene (*ACTB*) (±5,909) *vs.* 3,679 (±3,399), $p = 0.011$; *HPCA*: 5.31 (±3.24) *vs.* 2.95 (±2.67), $p = 0.012$), whereas no significant differences were observed for *DAG* (14,296.8 (±10,075.6) *vs.* 13,427.8 (±10,461.9), $p = 0.786$) (Supporting Information S4).

Similar results were obtained for fascin1 and hippocalcin immunohistochemical expression (Table 3, Fig. 1). Fascin1 expression was more frequent in SAC than in CC (88.6% *vs.* 14.3%; $p = 0.0001$). Similarly, hippocalcin had significantly greater expression in SAC than in CC (88.6% *vs.* 50%; $p < 0.0001$). No significant differences were observed for β-dystroglycan (Table 3).

Association of fascin1 and hippocalcin expression with oncogene mutations and MSI status

Results on *BRAF, KRAS* and *PIK3CA* mutations and MSI status were previously published.[8] Fascin1 expression was not statistically associated with MSI status ($p = 0.093$) but correlated with MGMT expression ($p = 0.002$), *BRAF* ($p = 0.002$) and *KRAS* ($p = 0.008$) mutation (Table 4). When restricting the analysis to SAC, fascin1 positivity was associated with *KRAS* mutation ($p = 0.030$) but not when restricted to CC ($p = 0.544$) (Supporting Information S5).

Correlation of hippocalcin and NAIP expression in different subtypes of colorectal carcinoma

Since the antiapoptotic activity of hippocalcin seems to be exerted through its interaction with NAIP[18] we decided to study its expression in our colorectal specimens. Supporting Information S6A shows the strong association of hippocalcin and NAIP expression in SAC, CC, hMSI-H CRC and in the whole study cases (0.002, <0.0001, 0.008 and <0.0001, respectively).

Predictive model for SAC diagnosis compared with CC based on immunohistochemical and molecular findings

Performance characteristics of the markers studied are described in Supporting Information S6B. The largest AUC-ROC was obtained for fascin1 (0.871) with a diagnostic odds ratio of 46.50 followed by hippocalcin (0.693) both showing the same sensitivity (88.6%). Of note, when considering marker combinations, 100% sensitivity was obtained for the positivity of at least one of these two markers. Both gave a high specificity (92.9%) which increased to 94.3% when MGMT loss was also considered.

Table 2. Differentially expressed mRNAs between serrated adenocarcinoma and conventional carcinoma obtained from molecular profile analysis

Probe	Symbol	Gene name and protein function[1]	Statistic	Fold change	Raw. *p* value	Adj. *p* value
A_24_P791862	A_24_P791862	UniGene Hs.680505	11.031	0.545	1.29 E −14	3.84 E −10
NM_003088	*FSCN1*	Fascin homolog 1. Actin-bundling protein. Organization of F-actin into parallel bundles. Formation of actin-based cellular protrusions. Role in cell migration, motility, adhesion, and cellular interactions.	6.167	1.529	1.52 E −07	0.0029
AF279773	LOC349160	Hypothetical. Similar: 60S ribosomal protein L18	5.986	0.444	2.86 E −07	0.0028
A_24_P934826	A_24_P934826	NCRNA00051 nonprotein coding RNA 51	5.883	0.472	4.09 E −07	0.003
THC2539939	THC2539939		5.242	2.647	3.72 E −06	0.019
NM_004393	*DAG1*	Dystroglycan 1. Laminin binding component of the dystrophin-glycoprotein complex. Linkage between the subsarcolemmal cytoskeleton and the extracellular matrix	5.177	0.883	4.64 E −06	0.019
NM_002143	*HPCA*	Hippocalcin. Neuron-specific calcium-binding protein. Regulation of photosignal transduction in a calcium-sensitive manner	5.085	1.156	6.35 E −06	0.023
NM_025250	*TTYH3*	Tweety homolog 3 (Drosophila). Calcium(2+)-activated large conductance chloride(−) channel	5.041	0.882	7.38 E −06	0.023
NM_001099	*ACPP*	Acid phosphatase, prostate. Conversion of orthophosphoric monoester to alcohol and orthophosphate. An isoform localized in the plasma membrane-endosomal-lysosomal pathway	4.986	2.159	8.87 E −06	0.024
NM_005094	*SLC27A4*	Solute carrier family 27. Fatty acid transport protein. Principal fatty acid transporter in enterocytes	4.985	1.062	8.92 E −06	0.024
NM_002196	*INSM1*	Insulinoma-associated 1. Protein containing both a zinc finger DNA-binding domain and a putative prohormone domain. Sensitive marker for neuroendocrine differentiation of human lung tumors	4.918	1.747	1.12 E −05	0.027
NM_032799	*ZDHHC12*	Zinc finger, DHHC-type containing 12. Membrane-associated protein. Metal ion binding, transferase activity of acyl groups.	4.772	0.879	1.82 E −05	0.036
A_24_P324488	*A_24_P324488*	SUGT1 SGT1. suppressor of G2 allele of SKP1 (*Saccharomyces cerevisiae*)	−4.870	−0.611	1.31 E −05	0.027
U66046	LOC100272228	LOC100272228 hypothetical LOC100272228	−4.886	−0.628	1.24 E −05	0.028
NM_024620	*ZNF329*	Zinc finger protein 329. Nuclear-associated protein. DNA and metal ion binding involved in regulation of transcription	−5.186	−1.244	4.51 E −06	0.020

[1]Source: http://www.ncbi.nlm.nih.gov/gene.

Survival analysis

Fascin1 positive expression was associated with a poorer outcome ($p = 0.003$). but there was no association with that of hippocalcin ($p = 0.17$) although survival at 60 months was worse in those positive for hippocalcin (37% *vs.* 53%) (Supporting Information S7). Multivariate analysis only identified SAC (*vs.* CC) (HR = 1.8 (CI 95%: 1.2–2.9); $p = 0.01$) and Dukes' C (*vs.* A/B) (HR = 2.6

Table 3. Immunohistochemical validation of the selected markers in SAC, CC, and MSI-H CRC

		Fascin1			Hippocalcin			β-Dystroglycan		
	n	Positive	Negative	*p*	Positive	Negative	*p*	Positive	Negative	*p*
SAC, *n* (%)	70	62 (88.6)	8 (11.4)		62 (88.6)	8 (11.4)		35 (50)	35 (50)	
CC, *n* (%)	70	10 (14.3)	60 (85.7)	<0.0001[1]	35 (50)	35 (50)	<0.0001[1]	34 (48.6)	36 (51.4)	0.500[1]
MSI-H CRC, *n* (%)	20	10 (50)	10 (50)	0.0001[2]	8 (40)	12 (60)	<0.0001[2]	10 (50)	10 (50)	1[2]

[1]SAC *versus* CC. [2]SAC *versus* MSI-H CRC.
Abbreviations: SAC: serrated adenocarcinoma; CC: conventional carcinoma; MSI-H CRC: high-level microsatellite unstable colorectal carcinoma.

Table 4. Association of immunohistochemical expression of fascin1, hippocalcin, and β-dystroglycan with CRC molecular markers in the study population

		MSI		MGMT		*BRAF*		*KRAS*		*PIK3CA*	
		MSI-H	MSI-L/MSS	Positive	Negative	Native	Mutated	Native	Mutated	Native	Mutated
Fascin	Positive	7 (11.1)	56 (88.9)	24 (42.9)	32 (57.1)	49 (77.8)	14 (22.2)	30 (47.6)	33 (52.4)	57 (90.5)	6 (9.5)
	Negative	2 (3.4)	57 (96.6)	39 (72.2)	15 (27.8)	57 (96.6)	2 (3.4)	42 (71.2)	17 (28.8)	53 (89.8)	6 (10.2)
	p		0.0931		0.0017		0.0017		0.0067		0.905
Hippocalcin	Positive	8 (9.8)	74 (90.2)	37 (50.7)	36 (49.3)	69 (84.1)	13 (15.9)	46 (56.1)	36 (43.9)	75 (91.5)	7 (8.5)
	negative	1 (2.5)	39 (97.5)	26 (70.3)	11 (29.7)	37 (92.5)	3 (7.5)	26 (65.0)	14 (35.0)	35 (87.5)	5 (12.5)
	p		0.150		0.049		0.192		0.3479		0.490
β-dystroglycan	Positive	4 (7.7)	48 (92.3)	32 (59.3)	22 (40.7)	50 (87.7)	7 (12.3)	29 (51.8)	27 (48.2)	51 (91.1)	5 (8.9)
	Negative	5 (7.1)	65 (92.9)	31 (55.4)	25 (44.6)	56 (86.2)	9 (13.8)	43 (65.2)	23 (34.8)	59 (89.4)	7 (10.6)
	p		0.909		0.679		0.798		0.0949		0.756

Abbreviations: MSI: microsatellite instability; MSI-H: high-level MSI; MSI-L: low-level MSI; MSS: microsatellite stability.

(CI 95%: 1.6–4.2); $p < 0.001$) as independent prognostic markers.

Comparison between SAC and hMSI-H CRC

Immunohistochemical fascin1 expression was more frequent in SAC than in hMSI-H CRC (88.6% *vs.* 50%; $p = 0.0001$). Similarly, hippocalcin was more frequently expressed in SAC than in hMSI-H CRC (88.6% *vs.* 40%; $p < 0.0001$). On the contrary, expression of β-dystroglycan was observed equally in both tumor types ($p > 0.05$). In the discrimination of SAC from hMSI-H CRC, the largest AUC-ROC was seen with hippocalcin (0.743) followed by fascin1 (0.693), both showing the same sensitivity (88.6%). When considering marker combinations, the positivity of fascin1 or hippocalcin gave a sensitivity of 100% for SAC diagnosis whereas the positivity for both showed a specificity of 80% (Supporting Information S6C). Distal (*vs.* proximal) location was the only independent prognostic factor identified for a poorer outcome (HR 1.9 (CI 95%: 1.1–3.2); $p = 0.02$).

Discussion

Microarray expression profiling is an excellent tool for identifying useful diagnostic, prognostic and predictive markers. However, given the amount of data made available for analysis, the results must be interpreted with caution and not only is validation mandatory but also the evaluation of these results in the context of currently available knowledge.

SAC is an emerging CRC tumor subset and previous studies have shown differences between it and CC with regard to morphology, presence of histological prognostic factors, immunohistochemical expression and molecular findings.[4–9] However, only one study has so far analyzed its expression profile ($n = 8$) compared with CC ($n = 29$).[12] Whilst our study has shown some interesting similarities, it differs in two important aspects: first, the tumor samples in our series were procured from patients with different genetic and environmental backgrounds and, second, a different microarray platform was used. Morphogenesis-, membrane- and hypoxia-related functions (such as VEGF signaling) were differentially expressed in SAC and CC in both studies. The observed differences in DNA repair gene expression may be explained by impairment of these proteins which characterizes the CIMP phenotype reported in SAC.[9] In some respects our results are consistent with those found in our previous studies: first, the immune-related functions (B-cell signaling, Fc receptor pathways) could be associated with a weaker peritumoral lymphocytic response which we found in SAC;[6] second, the cytoskeleton-related function and cell components here are consistent with the serrated morphology, the conspicuously invasive histological features of SAC[6] and the different expression pattern of proteins involved in the Wnt/beta-catenin pathway, actin binding and cell adhesion.[7]

Although the number of functions differently expressed in SAC and CC is considerable, we could only detect a

few differentially expressed genes. These, however, seem to be a distinctive and predictive feature of SAC diagnosed by immunohistochemistry. In the study by Laiho *et al.*,[12] the number of genes was much larger and a possible reason may be the different array platform used and a lower magnitude of the gene expression differences that may result in loss of significance after multiple-testing correction.

However, given the important and significant functions found by FatiScan in the present study, a clear coordinated transcriptional response that targets specific cellular functions is suggested. Moreover, the aforementioned strong predictive power of the differentially expressed genes detected indicates a high consistency in the major transcriptional differences between the two tissue types. Another possible reason for these differences could be that, in contrast with Laiho *et al.*,[12] our SAC and CC cases were also matched for the presence of mucinous component.

According to our microarray study, fascin1, hippocalcin and β-dystroglycan were the most differentially expressed genes between SAC and CC. Fascin1 protein localizes to the core actin bundles of spikes and filopodia at the leading edge of migratory cells and has been shown to increase migration in several cell types.[19] In fact, we observed that GO cellular components related to filopodium and lamelipodium were overrepresented in SAC. Several reports have demonstrated that in different epithelial tissues, fascin1 is absent in normal epithelium but present in tumors of the same tissue origin.[20] Our results are in agreement with those of Qualtrough *et al.*[21] who observed increased cell motility in colorectal adenoma cell lines following fascin transfection and with our previous results showing that SAC has a more active invasive front with fully recognized histological manifestations of epithelial-mesenchymal transition (EMT) such as tumor budding and cytoplasmic pseudofragments,[6] and with less expression of E-cadherin epithelial marker and an increase in the stromal marker laminin 5γ2.[7] Breast tumors also show upregulation of fascin1 and other proteins involved in extracellular matrix remodeling, invasion and EMT such as laminin, together with reduction of E-cadherin, this profile being associated with the basal-like phenotype characterized by an adverse prognosis.[22] We have observed that fascin1 expression is associated with shorter survival as has been reported previously in CRC[23] and all these findings may explain earlier observations showing that SAC fares worse than CC.[4] Moreover, the correlation between fascin1 expression and *KRAS* mutation indicates a possible predictive value since *KRAS* mutated CRC does not benefit from anti-EGFR therapies. In contrast, migrastatin analogues such as macroketone have been shown to inhibit metastatic tumor cell migration, invasion and metastasis through fascin blockade[24] thereby suggesting a potential specific role for migrastatin analogues in SAC treatment.

Hippocalcin is a calcium-sensor protein of the recoverin family[25] and when intracytoplasmic calcium levels increase, it is myristoylated and translocated to lipid membranes.[25,26] Amongst its functions, it seems to protect neurons against calcium-induced cell death.[18] Apoptotic evasion was one of the earliest features characteristic of SAC and has been suggested as the cause of its serrated morphology in which the transformed epithelium proliferates laterally adopting a sawtooth growth pattern.[1,5] Therefore, it is not surprising that hippocalcin is more expressed in SAC than in CC. Despite the fact that an aberrant expression of recoverin members has been reported in tumor cells,[27] no previous reports have described the presence of hippocalcin in CRC. Although hippocalcin expression in CRC is small at the mRNA level, we have demonstrated it with three different techniques and, moreover we found differentially expressed functions in SAC related to hippocalcin (apoptosis, calcium regulation and neural morphogenesis). Since the antiapoptotic activity of hippocalcin seems to be exerted through its interaction with NAIP,[18] we found in our study of its expression in our CRC specimens that hippocalcin and NAIP are strongly correlated, both showing a granular cytoplasmic staining. All these findings support the hypothesis that hippocalcin may play a causative role in SAC development although further functional studies are necessary to characterize its role in colorectal carcinogenesis. Several genes overexpressed in SAC are neural-related including not only hippocalcin but also INSM1, a sensitive marker for neuroendocrine differentiation of human lung tumors.[28] Similarly, the transcript THC2539939 is overexpressed in metastases and not in primary gastroenteropancreatic neuroendrocrine tumors.[29]

Data on differentially expressed functions and genes appear to show that SAC, unlike CC, has a characteristic profile of cytoskeletal rearrangement which could be responsible for special cell adhesion and invasive properties. In addition, specific activation of pathways involving small GTPases and lipidic second messengers as phosphatidylinositols could be implicated in this process. It is important to highlight the role of phosphatidylinositol trisphosphate and the small GTPases RAC and CDC42 in the actin assembly for lamelipodia and filopodia organization.[30]

The identification of reliable markers is not only useful for SAC diagnosis but it may also help to know which type of adenoma is the SAC precursor lesion. Three immunohistochemical markers have been proposed for SAC diagnosis, HIF1α being the most discriminant between SAC and CC with a positivity of 62.2% and 21.7%, respectively[12] and similar percentages for HIF1α were obtained in a subset of our series (data not shown). In our study, the positive expression of fascin1 was observed in 88.6% of SAC and in 14.3% of CC (88.6% sensitivity, 85.7% specificity). Of note, the positivity of fascin1 or hippocalcin increased sensitivity to 100% indicating that when both markers are negative it is highly unlikely that a given tumor is a SAC. It has been suggested that MGMT loss is typical of SAC[8] and the addition of MGMT loss to fascin1 and hippocalcin positivity increases the specificity to 94.3% but with lower sensitivity (54.3%).

Most MSI-H CRC are sporadic.[10] MSI-related histology was first introduced in the Revised Bethesda Guidelines[31] in order to facilitate the diagnosis of some later-onset CCR with "likely Lynch syndrome" with little or no other suggestive personal or family history. However, there is no histologic feature that could distinguish Lynch syndrome CRC from sporadic MSI-H CRC and several studies have confirmed that tumor histology was a better predictor of MSI-H CRC than was personal and family history of cancer and, according to this, several histology-based models have been proposed for predicting MSI in CRC irrespective of its familiar or sporadic origin.[32–35]. SAC and MSI-H CRC account for similar percentages amongst CRC subsets, but, whereas CRCs showing hMSI-H CRC have a molecular marker for its confirmation (MSI testing), no specific marker for SAC has so far been reported. It has recently been shown that SAC are mostly *KRAS*- or *BRAF*-mutated and not MSI-H tumors[8,9] although, compared with CC, it can share several MSI-H CRC characteristics such as *BRAF* mutation, MSI-H, CIMP and proximal colon location. It could be possible that some serrated polyps be the precursors of hMSI-H CRC and SAC. The histological differences between both tumors could be attributed to two divergent molecular routes, one driven by BRAF and the other by KRAS mutations. It was for these reasons that we decided to investigate if fascin1 and hippocalcin could also help to discriminate SAC from hMSI-H CRC. Again, both fascin1 and hippocalcin expression were significantly associated with SAC diagnosis hippocalcin showing slightly better performance characteristics when distinguishing SAC from hMSI-H CRC with the positivity of one of them being highly predictive of SAC.

In conclusion, fascin1 and hippocalcin can be regarded as useful immunohistochemical adjuncts for SAC diagnosis and may be playing an important role in the biology and clinical behavior of SAC. The functional characterization of these molecules in this context and their evaluation in serrated adenomas may shed further light on the serrated pathway.

Acknowledgements

The authors are grateful to Isabel Molina for technical assistance and to Dr. Mike Tobin for English proof reading.

References

1. Hamilton SR, Bosman FT, Boffetta P, et al. Carcinoma of the colon and rectum. In: Bosman FT, Carneiro F, Hruban RH, et al., eds. WHO classification of tumors of the digestive system. Lyon: IARC, 2010. 134–46.
2. Mäkinen MJ, George SM, Jernvall P, et al. Colorectal carcinoma associated with serrated adenoma--prevalence, histological features, and prognosis. *J Pathol* 2001;193:286–94.
3. Tuppurainen K, Mäkinen JM, Junttila O, et al. Morphology and microsatellite instability in sporadic serrated and non-serrated colorectal cancer. *J Pathol* 2005;207:285–94.
4. García-Solano J, Pérez-Guillermo M, Conesa-Zamora P, et al. Clinicopathologic study of 85 colorectal serrated adenocarcinomas: further insights into the full recognition of a new subset of colorectal carcinoma. *Hum Pathol* 2010;41:1359–68.
5. Mäkinen MJ. Colorectal serrated adenocarcinoma. *Histopathology* 2007;50:131–50.
6. García-Solano J, Conesa-Zamora P, Trujillo-Santos J, et al. Tumor budding and other prognostic pathological features at invasive margins in serrated colorectal adenocarcinoma: a comparative study with conventional carcinoma. *Histopathology* 2011;59:1046–56.
7. García-Solano J, Conesa-Zamora P, Trujillo-Santos J, et al. Immunohistochemical expression profile of β-catenin, E-cadherin, P-cadherin, laminin-5γ2 chain, and SMAD4 in colorectal serrated adenocarcinoma. *Hum Pathol*, 2012;43: 1094–102.
8. García-Solano J, Conesa-Zamora P, Carbonell P, et al. Colorectal serrated adenocarcinoma shows a different profile of oncogene mutations, MSI status and DNA repair protein expression compared to conventional and sporadic MSI-H carcinomas. *Int J Cancer*, doi: 10.1002/ijc.27454.
9. Stefanius K, Ylitalo L, Tuomisto A, et al. Frequent mutations of KRAS in addition to BRAF in colorectal serrated adenocarcinoma. *Histopathology* 2011;58:679–692.
10. Huang CS, Farraye FA, Yang S, et al. The clinical significance of serrated polyps. *Am J Gastroenterol* 2011;106:229–40.
11. O'Brien MJ, Yang S, Mack C, et al. Comparison of microsatellite instability, CpG island methylation phenotype, BRAF and KRAS status in serrated polyps and traditional adenomas indicates separate pathways to distinct colorectal carcinoma end points. *Am J Surg Pathol* 2006;30: 1491–501.
12. Laiho P, Kokko A, Vanharanta S, et al. Serrated carcinomas form a subclass of colorectal cancer with distinct molecular basis. *Oncogene* 2007;26: 312–20.
13. Redston M. Epithelial neoplasms of the large intestine. In: Odze RD, Goldblum JR, Crawford JM, eds. Surgical pathology of the GI tract, liver, biliary tract, and pancreas. Philadelphia: Saunders, 2004. 441–72.
14. Bellizzi AM, Frankel WL. Colorectal cancer due to deficiency in DNA mismatch repair function: a review. *Adv Anat Pathol* 2009;16:405–17.
15. Benjamini Y, Hochberg Y. Controlling the false discovery rate: a practical and powerful approach to multiple testing. *J R Stat Soc B* 1995;57: 289–300.
16. Al-Shahrour F, Carbonell J, Minguez P, et al. Babelomics: advanced functional profiling of transcriptomics, proteomics and genomics experiments. *Nucleic Acids Res* 2008;36: W341–W346.
17. Jiang X, Rieder S, Giese NA, et al. Reduced alpha-dystroglycan expression correlates with shortened patient survival in pancreatic cancer. *J Surg Res* 2011;171:120–126.
18. Mercer EA, Korhonen L, Skoglösa Y, et al. NAIP interacts with hippocalcin and protects neurons against calcium-induced cell death through caspase-3-dependent and -independent pathways. *EMBO J* 2000;19:3597–607.
19. Kureishy N, Sapountzi V, Prag S, et al. Fascins, and their roles in cell structure and function. *Bioessays* 2002;24:350–61.
20. Hashimoto Y, Skacel M, Adams JC. Roles of fascin in human carcinoma motility and signalling: prospects for a novel biomarker. *Int J Biochem Cell Biol* 2005;37:1787–804.
21. Qualtrough D, Singh K, Banu N, et al. The actin-bundling protein fascin is over-expressed in colorectal adenomas and promotes motility in adenoma cells in vitro. *Br J Cancer* 2009;101:1124–9.
22. Sarrió D, Rodriguez-Pinilla SM, Hardisson D, et al. Epithelial-mesenchymal transition in breast cancer relates to the basal-like phenotype. *Cancer Res* 2008;68:989–97.
23. Hashimoto Y, Skacel M, Lavery IC, et al. Prognostic significance of fascin expression in advanced colorectal cancer: an immunohistochemical study of colorectal adenomas and adenocarcinomas. *BMC Cancer* 2006;6:241.
24. Chen L, Yang S, Jakoncic J, et al. Migrastatin analogues target fascin to block tumour metastasis. *Nature* 2010;464:1062–6.
25. Kobayashi M, Takamatsu K, Saitoh S, et al. Myristoylation of hippocalcin is linked to its calcium-dependent membrane association properties. *J Biol Chem* 1993;268:18898–904.
26. Callaghan DW, Tepikin AV, Burgoyne RD. Dynamics and calcium sensitivity of the Ca2+/ myristoyl switch protein hippocalcin in living cells. *J Cell Biol* 2003;163:715–21.
27. Miyagawa Y, Ohguro H, Odagiri H, et al. Aberrantly expressed recoverin is functionally associated with G-protein-coupled receptor kinases in cancer cell lines. *Biochem Biophys Res Commun* 2003;300:669–73.
28. Lan MS, Breslin MB. Structure, expression, and biological function of INSM1 transcription factor

in neuroendocrine differentiation. *FASEB J* 2009; 23:2024–33.
29. Posorski N, Kaemmerer D, Ernst G, et al. Localization of sporadic neuroendocrine tumors by gene expression analysis of their metastases. *Clin Exp Metastasis* 2011;28: 637–47.
30. Cavallaro U, Christofori G. Cell adhesion and signalling by cadherins and Ig-CAMs in cancer. *Nat Rev Cancer* 2004;4:118–32.
31. Umar A, Boland CR, Terdiman JP, et al. Revised Bethesda Guidelines for hereditary nonpolyposis colorectal cancer (Lynch syndrome) and microsatellite instability. *J Natl Cancer Inst* 2004;96:261–8.
32. Jenkins MA, Hayashi S, O'Shea AM, et al. Pathology features in Bethesda guidelines predict colorectal cancer microsatellite instability: a population-based study. *Gastroenterology* 2007;133:48–56.
33. Greenson JK, Huang SC, Herron C, et al. Pathologic predictors of microsatellite instability in colorectal cancer. *Am J Surg Pathol* 2009;33: 126–33.
34. Hyde A, Fontaine D, Stuckless S, et al. A histology-based model for predicting microsatellite instability in colorectal cancers. *Am J Surg Pathol* 2010;34:1820–9.
35. Bessa X, Alenda C, Paya A, et al. Validation microsatellite path score in a population-based cohort of patients with colorectal cancer. *J Clin Oncol* 2011;29:3374–80.